JJMIE

Volume 5, Number 2, April 2011
ISSN 1995-6665
Pages 119 - 128

Jordan Journal of Mechanical and Industrial Engineering

Inverse Design of Impeller Blade of Centrifugal Pump with a Singularity Method

Wen-Guang LI*

Department of Fluid Machinery, Lanzhou University of Technology, 287 Langongping Road, 730050 Lanzhou, China

Abstract

The singularity method has been extensively applied into an analysis of the potential flow through centrifugal pump impellers, i.e. direct problem, but it was little utilized in inverse design of such impeller blades, i.e. inverse problem. In this paper, a singularity method was applied for inversely designing impeller blades. A cubic Bezier curve was established to express mathematically density function of bound vortex intensity along the blade camber line so as to get a smooth and loading carefully controlled blade. The angle of attack and blade loading coefficient were taken into account in the given density function of bound vortex intensity. The direct and inverse problems have been validated with a typical experimental centrifugal pump impeller. Furthermore, the impeller blades were redesigned by using the method, and the three-dimensional turbulent viscous flows inside the original and redesigned impellers were calculated numerically by means of a CFD code Fluent. It was shown that the blade shape and flow pattern on the blade can be controlled easily by altering the density function of bound vortex intensity. The CFD outcomes confirmed that the original impeller hydraulic efficiency was improved by 5% at the design duty, but 9% at off-design condition.

Keywords: centrifugal pump; singularity method; impeller; blade; inverse problem; inverse design; CFD

1. Introduction*

The singularity method is an important numerical approach for numerically solving blade-to-blade potential flows within centrifugal impellers and has been substantially involved in the analysis of hydrodynamics of centrifugal pump impellers for years, for instance, Ayyubi and Rao [1], Reddy and Kar [2], Ogawa and Murata [3, 4], [5], Kumar and Rao [5, 6]. Unfortunately, this method was almost applied to solve a direct problem, rather than an inverse one for centrifugal impellers. Betz and Flugge-Lotz [7] initially proposed a singularity approach for inversely establishing radial impeller blades. They realized that a two-dimensional potential internal flow in a centrifugal impeller is a superposition of a uniform inflow at the impeller entrance and a non-uniform flow caused from a series of vortexes bound to the blade camber lines. The density of bound vortex intensity was assumed to be varied circumferentially by means of the Fourier series. An analytical equation for calculating the absolute velocity induced by those vortices at a point in the flow domain was derived. Kashiwabaray [8] expanded this method analytically to make it suitable to mixed-flow impellers. In his proposal, the blade shape was determined iteratively by using the prescribed fluid relative velocity profile on both sides of blade. A series of vortex and source (sink) were allocated simultaneously on the blade camber lines. The density of bound vortex intensity was determined numerically with the difference of the two prescribed velocity profiles and the length of camber line. The intensity of the source (sink) was given by using the blade thickness profile specified. Finally, a blade angle was calculated by means of the tangential condition, causing an updated blade shape. This process was redone unless the blade shape no longer was changed. This method was applicable to the centrifugal impellers with more number of blades (>7). Murata and Miyake et al [9] mapped a S1 stream-surface (blade-to-blade) of revolution onto a two-dimensional rectilinear cascade by using conformational mapping function twice. Similarly, a series of vortex and source (sink) were distributed on the blade camber line; then the densities of the bound vortex and source (sink) intensities were determined by using the relative velocity and blade thickness prescribed. The induced velocity equations in Murata and Miyake et al [9] were more general than those in Betz and Flugge-Lotz [7]. It is believed the blade shape control is hard in those two proposals since the relative velocity profile on both sides of blade must be prescribed together. They seem inconvenient for applications.

It is interesting to notice that a simple and smart singularity approach for solving the blade-to-blade

* Corresponding author. Liwg38@yahoo.com

potential flow on a revolutionary stream-surface was presented by Senoo and Nakase [10]. The method has found significant applications in the analysis of flow inside centrifugal impellers. Recently, it was upgraded with three kinds of density function of bound vortex intensity by Li [11] and was applied to analyze the potential flow in very low specific speed centrifugal pump impellers with various blades and splitters.

Based on this method, a singularity method for designing centrifugal pump impeller blades as an inverse problem has been developed in this paper. The objective is to clarify feasibility of the method for establishing blades and to identify if it can easily control the blade shape. The blade of an experimental centrifugal pump impeller was redesigned as an inverse problem. The hydraulic performance of the original and redesigned impellers was estimated numerically by using CFD code Fluent. As a consequence, more than 5% improvement in the hydraulic efficiency was confirmed.

2. Equations and Methods

2.1. Direct Problem

For convenience, a centrifugal pump impeller is assumed to rotate contraclockwise as it is viewed against its inlet (Fig. 1). The intensity of a contraclockwise bound vortex is assumed to be positive; otherwise, it is negative. Further, the blades of the impeller are curved backward. In that case, the blade angle β_b is positive, which is defined as the angle between a tangent to the blade camber line at a point on a S1 stream-surface of revolution and the reverse direction of impeller rotation at that point. Note that the angle $\beta_b - 90^\circ$ is negative, which is the angle between that tangent and the meridian plane through that point.

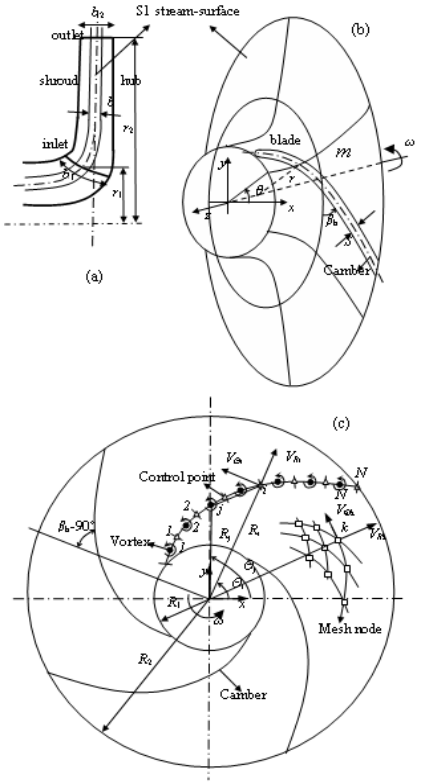

Figure 1.Impeller meridian plane (a) and S1 stream surface (physical surface) (b) as well as computational plane (c), where bound vortices are specified

For a direct problem, the number of blades, blade camber shape, blade thickness, S1 stream-surfaces of revolution and their thickness, the volumetric flow rate through the impeller and rotational speed etc have been known. The following steps are needed to analyze a two-dimensional ideal fluid flow in a centrifugal pump impeller by using the singularity method proposed initially by Senoo and Nakase [10] and updated by Li [11].

1. A S1 stream-surface of revolution in terms of the coordinates $m-\theta$ in the physical surface was mapped onto a circular cascade in terms of the polar coordinates $R-\Theta$ in the computational plane by using the Prasil transformation relations in Senoo and Nakase [10]

$$\begin{cases} R = R_1 e^{\int_0^m \frac{dm}{r}} \\ \Theta = \theta \end{cases} \tag{1}$$

The circular cascade has an inner R_1 and an outer radius R_2, in which $R_2 = R_1 exp\left(\int_0^{m_2} 1/r dm\right)$, m_2 is the length of the meridian streamline at the blade exit, r is the radius specifying the stream-surface. Every computation of the flow is carried out in the computational plane; once finished, it will be transformed back to the physical surface via Eq. (1).

2. A series of bound vortices are assumed to be distributed on a blade camber line, so the absolute velocity components induced by these vortices ($j = 1, 2, \ldots, N$) at an observed point i on the blade camber line or a point k in the flow domain in the computational plane are given as follows

$$\begin{cases} V_{\Theta i} = +\dfrac{Z}{4\pi R_i}\int_0^{s_2}(1-F_\Theta)\lambda ds \\ V_{Ri} = -\dfrac{Z}{2\pi R_i}\int_0^{s_2} F_R \lambda ds \end{cases} \tag{2}$$

And

$$\begin{cases} F_\Theta = \dfrac{\left(R_j/R_i\right)^Z - \left(R_j/R_i\right)^{-Z}}{\left(R_j/R_i\right)^Z + \left(R_j/R_i\right)^{-Z} - 2\cos\left[Z(\Theta_i - \Theta_j\right]} \\ F_R = \dfrac{\sin\left[Z(\Theta_i - \Theta_j\right]}{\left(R_j/R_i\right)^Z + \left(R_j/R_i\right)^{-Z} - 2\cos\left[Z(\Theta_i - \Theta_j\right]} \end{cases} \tag{3}$$

where s_2 is the length of blade camber line at the blade outlet, Z is the number of blades, λ is the density of bound vortex intensity, which is expressed in terms of the length of blade camber s. The velocity components $(V_{\Theta k}, V_{Rk})$ are for the point k in the flow domain.

3. Provided that the observed point i is on a blade camber line, the fluid relative velocity will be the tangent at this point, i.e. the relative flow angle β_i equals the blade angle β_{bi}. Eventually, a tangential condition is be satisfied

$$tan\left(\beta_i - 90^\circ\right) = \frac{W_{\Theta i}}{W_{Ri}} = tan\left(\beta_{bi} - 90^\circ\right) \tag{4}$$

The relative velocity components are related to the absolute velocity via the following equations

$$\begin{cases} W_{Ri} = V_{Ri} + \overline{W}_{Ri} \\ W_{\Theta i} = V_{\Theta i} - \overline{U}_i \end{cases} \quad (5)$$

The velocity components $\overline{W}_{Ri}$ and $\overline{U}_i$ are estimated by using the flow rate through the impeller and the pre-circulation in the impeller entrance as follows

$$\begin{cases} \overline{W}_{Ri} = \dfrac{Q}{b_i\left(2\pi R_i - ZS_{ui}\right)} \\ \overline{U}_i = \dfrac{1}{R_i}\left(v_{u1}r_1 - u_i r_i\right) \end{cases} \quad (6)$$

where Q is the flow rate across the impeller, b_i is the thickness of S1 stream-surface, the blade circumferential thickness is $S_{ui} = S_i / \sin\beta_{bi}$, S_i is the blade thickness on S1 stream-surface, $v_{u1}r_1$ is the absolute velocity moment at the impeller entrance, u_i is the impeller speed at the radius r_i, $u_i = r_i\omega$, ω is the angular rotational speed of impeller.

Putting Eq. (2) into (4), the tangential condition is rewritten as

$$\int_0^{s_2}\left(1 - F_\Theta\right)\lambda ds + 2\tan\left(\beta_{bi} - 90^\circ\right)\int_0^{s_2} F_R \lambda ds = \frac{4\pi R_i}{Z}\left(\overline{U}_i + \tan\left(\beta_{bi} - 90^\circ\right)\overline{W}_{Ri}\right) \quad (7)$$

This is a system of integral equations in terms of the unknown density of bound vortex intensity λ. In order to get a numerical solution of such an equation system, the continuous density λ needs to be discretized. Here, a continuous blade camber line is divided into small-sized segment elements with a number of N. The density of bound vortex intensity is considered to be constant in each element, but the density in one element may be different from that in another. It is assumed the bound vortex is located at the centre of each element. The intensity of a bound vortex j ($j = 1,2,3,\cdots,N$) is connected with its density via

$$\mu_j = \lambda_j ds_j \approx \lambda_j \Delta s_j \quad (8)$$

where Δs_j denotes the length of an element in which the vortex j is prescribed. Substituting λds in Eq. (7) with $\lambda_j \Delta s_j$ in Eq. (8), the system of integral equations becomes a system of linear algebraic equations in terms of λ_j

$$\left[\sum_{j=1}^{N}\left(1 - F_{\Theta j}\right) + 2\tan\left(\beta_{bi} - 90\right)F_{Rj}\right]\Delta s_j \lambda_j = \frac{4\pi R_i}{Z}\left(\overline{U}_i + \tan\left(\beta_{bi} - 90\right)\overline{W}_{Ri}\right) \quad (9)$$

where the point i is on the blade camber line, but it is the node with larger radius in an element. The tangential condition has been applied at that point, so the point i ($i = 1,2,3,\cdots,N$) is considered to be a control point. Note that the total number of control point i equals the number of elements N. In the last element near the blade trailing edge, the Kutta condition must be fulfilled, i.e. λ_N =0. In that case, the Eq. (9) represents a set of $N-1$ simultaneous linear algebraic equations in $N-1$ unknown variables.

4. Solve the system of linear equations (9) to determine the unknown λ_j.
5. The induced absolute velocity components in Eq. (2) at the point i on the blade camber line can be calculated by using the λ that has been determined. Subsequently, Eq. (5) is applied to figure out the relative velocity components W_{Ri}, $W_{\Theta i}$ on the blade pressure and suction sides as follows

$$\begin{cases} W_{si} = \sqrt{W_{Ri}^2 + W_{\Theta i}^2} + \dfrac{1}{2}\lambda_i \\ W_{pi} = \sqrt{W_{Ri}^2 + W_{\Theta i}^2} - \dfrac{1}{2}\lambda_i \end{cases} \quad (10)$$

6. Calculate the fluid relative velocity at specified points or a series of node of a mesh in the flow passage, if necessary. Otherwise, go to the next step.
7. The relative velocity components in the physical surface or S1 stream-surface in terms of the coordinates $m-\theta$ are obtained with the following transformation

$$\begin{cases} w_{ri} = \left(R_i / r_i\right)W_{Ri} \\ w_{\theta i} = \left(R_i / r_i\right)W_{\Theta i} \end{cases} \quad (11)$$

Finally, the Bernoulli equation can be utilized to get the pressure field in the flow passage to a reference pressure. Moreover, the theoretical head of impeller is predicted by

$$H_{th} = \left(\overline{v}_{u2}u_2 - v_{u1}u_1\right)/g \quad (12)$$

And the mean circumferential component of absolute velocity at the blade outlet is written as

$$\overline{v}_{u2} = u_2 - \frac{Z}{2\pi \overline{w}_{m2}}\int_0^{\frac{2\pi}{Z}} w_{u2}w_{m2}d\theta \quad (13)$$

where the mean meridian component of relative velocity at the blade outlet is

$$\overline{w}_{m2} = \frac{Z}{2\pi}\int_0^{\frac{2\pi}{Z}} w_{m2}d\theta \quad (14)$$

The slip factor is expressed as

$$\sigma = \frac{Z}{2\pi u_2 \overline{w}_{m2}}\int_0^{\frac{2\pi}{Z}} w_{u2}w_{m2}d\theta - \frac{Q}{u_2 b_2\left(2\pi r_2 - ZS_{u2}\right)\tan\beta_{b2}} \quad (15)$$

2.2. Inverse Problem

For an inverse problem in the singularity method, the number of blades, blade thickness profile, blade leading and trailing edge shapes and positions, S1 stream-surface shape and thickness, flow rate through an impeller and rotating speed of the impeller have been known in advance; just the blade camber line needs to be determined.

Usually, the blade camber line is represented by a relation of radius to warping angle or vice versa. How to establish such a relation is a key issue in the inverse problem. In most cases, a correct relation has to be achieved iteratively based on an initially guessed one. In this paper, the following steps are conducted to get a proper blade camber line.

1. Specify a temporary distribution of blade angle β_b^0 along a meridian streamline from the blade leading edge to trailing edge, subsequently, a relation of initial wrapping angle of blade with r can be established by integrating the blade pattern equation as follows

$$\theta = \int_0^{m2}\frac{\tan\left(\beta_b - 90^\circ\right)}{r}dm \quad (16)$$

For the sake of convenience, the initial blade usually is radial, i.e. $\beta_b = 90^0$. Eq. (16) is numerically integrated by simply applying the trapezium rule. Once the initial

relation $\theta - r$ is available, the initial blade will be mapped onto the computational plane with Eq. (1).

2. Prescribe a profile of density of bound vortex intensity on the blade camber line. A cubic Bezier curve in Rogers [12] is utilized to describe the density of bound vortex intensity to guarantee a sufficient smooth blade camber line achievable. Such a curve is defined by a control polygon with four control vertices A, B, C and D as shown in Fig. 2. Then the density of bound vortex intensity is expressed mathematically as

$$\lambda(s) = (1-t)^3\lambda_a + 3t(1-t)^2\lambda_b + 3t^2(1-t)\lambda_c + t^3\lambda_d \quad (17)$$

where the parameter $t = (s - s_a)/(s_d - s_a)$, $\lambda_b = c\lambda_a$, $\lambda_c = d\lambda_a$, factors c and d are adjustable to correlate λ_a.

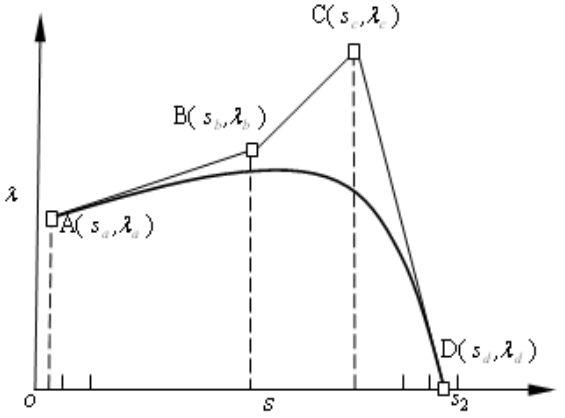

Figure 2.A cubic Bezier curve is used to define density distribution of bound vortex on blade

Firstly, the initial blade camber is divided into N elements equally, and the length of each element is Δs. At point D, the Kutta condition must be yielded, so the coordinates of D are $s_s = s_2 - \Delta s/2$, $\lambda_d = 0$. At point A, $s_a = 0.5\Delta s$, the intensity λ_a is determined such a way that a proper angle of attack α must be realized. In doing so, a relative flow angle β_1 to the blade leading edge is estimated as follows

$$\beta_1 = tan^{-1}\left(\frac{v_{m1}}{u_1 - v_{u1}}\right) \quad (18)$$

and the meridian velocity component at the leading edge is given by

$$v_{m1} = \frac{Q}{(2\pi r_1 - ZS_{u1})b_1} \quad (19)$$

Secondly, a proper angle of attack is specified. If the impeller is expected to have a better cavitation performance, then α=0.5°-3°; otherwise, α=3°-5°. In consequence, the blade angle at the inlet is $\beta_{b1} = \beta_1 + \alpha$. Because of $r_1 \approx r_a$ (radius at point A), then $\beta_{b1} \approx \beta_{ba}$, $u_1 \approx u_a$ and $v_{m1} \approx v_{ma}$. Subsequently, the circumferential component of absolute velocity at point A is written as

$$v_{ua} = u_1 - \frac{v_{m1}}{tan\,\beta_{b1}} \quad (20)$$

Finally, the density of bound vortex intensity at point A is given by

$$\lambda_a = \frac{2\pi r_a (v_{ua} - v_{u1})}{Z\Delta s} \quad (21)$$

Points B and C are used to control the peak value of the density and its position on the blade camber line. Usually, $s_b \in [0.3(s_d - s_a) + s_a, 0.5(s_d - s_a) + s_a]$ and $s_c \in [0.8(s_d - s_a) + s_a, 0.95(s_d - s_a) + s_a]$. The densities λ_b, λ_c are specified with two factors b and c as well as λ_a, but they are subject to two critical conditions: (a) the peak loading coefficient (velocity gradient) on the blade is less than 2, i.e. $\Delta W/W \le 2$ to avoid a reverse flow on the blade pressure side in Balje [13], where $\Delta W = W_s - W_p$, W_s is the relative velocity on blade suction side, W_p that on blade pressure side, $W = 0.5(W_s + W_p)$; (b) make sure the theoretical head developed by the designed impeller must be over the head desired.

3. Calculate the relative velocity components $W_{\Theta i}$, W_{Ri} by using Eqs. (2), (3), (5), (6) with the specified density profile of bound vortex intensity, the blade angle β_{bi} is updated with Eq. (4).
4. Integrate Eq. (16) once more by applying the updated blade angle β_{bi}. In consequence, the relation between blade warping angle and blade angle is upgraded and a new blade camber line is generated. This computational process isn't stopped until the blade camber line shows little change in its shape. The blade camber line convergence criterion is the relative error (difference of warping angle over the mean value between two successive iterations) is less than 1×10^{-3}.
5. Calculate the relative velocities in the flow passage with Eqs. (2,3, 5 and (6) and transform those velocities into the physical surfaces with Eq. (11). Finally, the impeller theoretical head and slip factor etc are estimated by using Eqs. (12-15).
6. If these primary hydraulic parameters are satisfactory, then this inverse design process will be terminated. Otherwise, a new design should be launched with a modified density profile of bound vortex intensity or other design variables. Nevertheless, the steps (1)-(5) will be carried out until a satisfactory result is achieved.
7. Generate the three-dimensional solid geometry model of the impeller just established and launch CFD stimulations of viscous fluid flow inside the impeller to make sure the impeller has shown a perfect performance and pretty well flow patterns. Otherwise, necessary corrections should be applied to the design variables and a new inverse design is started by following the steps (1) to (5).

3. Results and Discussions

3.1. Direction Problem Validation

In order to validate the method proposed, the ideal fluid flow in the experimental impeller presented in Kamimoto and Hirai [14] was analyzed by using the method. The duty of the impeller at design condition is as follows: Q =287m^3/h, head H =26m, rotating speed n =1750r/min, specific speed n_s =156 ($n_s = 3.65n\sqrt{Q}/H^{0.75}$, r/min, m^3/s, m), impeller tip speed u_2 =27.5m/s, flow coefficient $\phi = Q/2\pi r_2 b_2 u_2$ =0.154 and head coefficient $\psi = gH/u_2^2$ =0.34. The geometrical parameters of the impeller as the following: impeller outlet diameter D_2 =300mm, impeller eye diameter D_e =150mm. Four constant-width (b=20mm), constant-thickness (S=3mm), constant-angle (β_b =30°) logarithmic spiral blades were installed in the shrouded radial impellers. In spite of a bit high specific speed, the blades were two-dimensional and

without twist along blade span for convenience in experiments in Kamimoto and Hirai [14]. Since this experimental impeller serves a benchmark in the paper, it is not intended to design a new impeller with twist blades. This means the ideal flow analysis and blade redesign were conducted just on one S1 stream-surface of revolution.

The effect of number of elements of discretized bound vortices N on the impeller theoretical head coefficient ψ is shown in Fig. 3. The number of elements does affect the head coefficient moderately; fortunately, this effect is negligible as the number more than 60. In that case, the length of element is around 2.5mm. In the following computations, the number of element is kept to be 60.

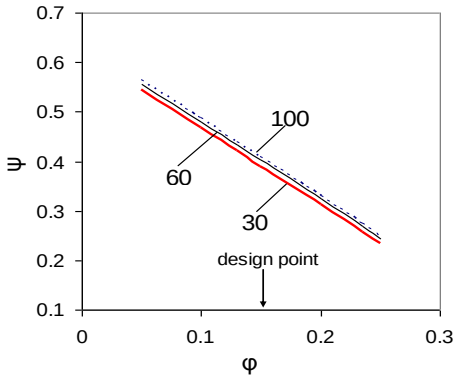

Figure 3.Impeller theoretical head against flow coefficient at various numbers of vortex elements.

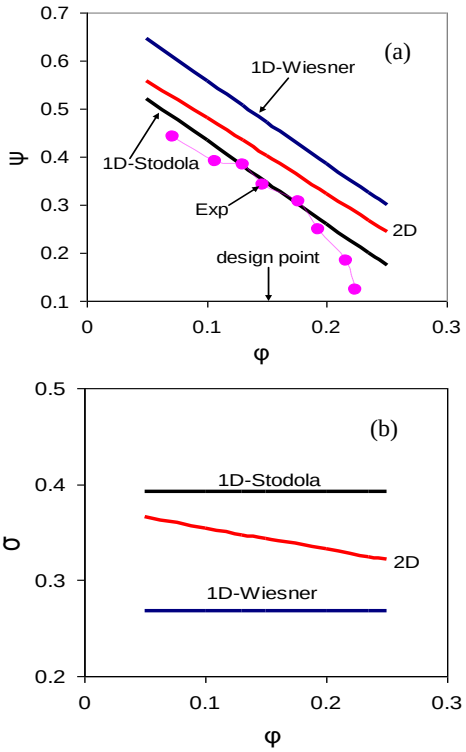

Figure 4.Impeller theoretical head coefficient and slip factor in terms of flow coefficient, the symbols represent experimental data in Kamimoto and Hirai [14].

The impeller theoretical head ψ, which was determined by using the 2D singularity method, is plotted in terms of flow rate coefficient ϕ in Fig. 4a. The head coefficients evaluated by means of the one-dimensional (1D) Euler turbomachinery head equation with respective corrections of Stodola and Wiesner slip factors are also shown in the figure. The experimental head coefficient in Kamimoto and Hirai [14] is involved in the plot as well. A comparison of 2D computed slip factor to those of Stodola and Wiesner is made in Fig. 4b. The head coefficient given by 2D singularity approach is in between those of the 1D Euler head plus slip factor correction. The slip factor due to the 2D singularity method is in between those of Stodola and Wiesner too. These facts suggest the results provided by 2D singularity method seems reasonable.

Figure 5 illustrates the fluid relative velocities on the blade pressure and suction surfaces as well as blade loading coefficient $\Delta W/W$ in terms of dimensionless blade camber line length. On the suction surface, the relative velocity of the 2D singularity method is fairly close to the experimental profile. On the pressure surface, however, the velocity is much lower than the experimental observation; further, at the nearby r/r_2 =0.55 location, i.e. just behind the blade leading edge, the relative velocity has become zero, causing a maximum difference of velocity between the suction and pressure surfaces. Accordingly, the blade loading coefficient in Fig. 5b has also got a maximum value there. Note that this peak value has been as large as 2. It was indicated that once $\Delta W/W$ =2, a fluid flow would be separated from the blade pressure side by Balje [13]. Obviously, the computed peak loading factor is in very good agreement with such an observation. This suggests the experimental impeller has been subject to an extreme high hydrodynamic loading.

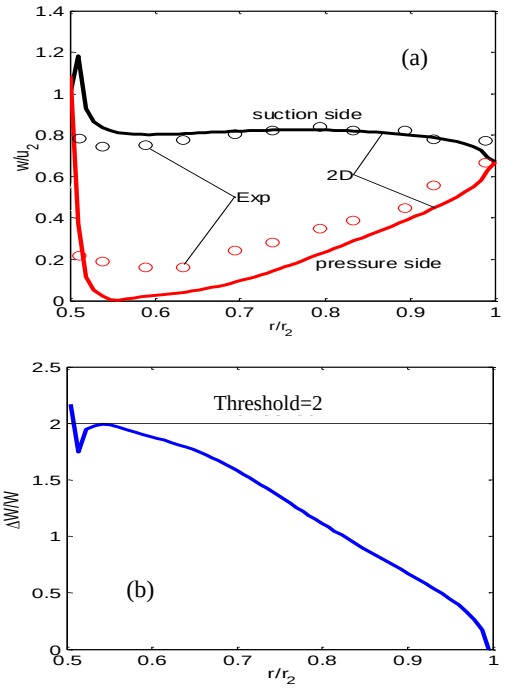

Figure 5.Relative velocity profile and blade loading coefficient on blade pressure and suction surfaces against dimensionless length of blade, the symbols indicate the experimental measurements.

For the 2D singularity method is based on an ideal fluid flow model, there is not a boundary layer in the impeller passages, causing no any hydraulic losses there. This effect causes the estimated impeller theoretical head coefficient

to be higher than the observation (see Fig. 4a). Such a flow model exaggerates the relative velocity difference between the blade suction and pressure sides, i.e. blade loading or hydrodynamic loading. A much under-estimated velocity on the blade pressure surface is responsible for the exaggerated difference. The ignored viscous and three-dimensional effect may be responsible for the disagreement in the impeller head coefficient and relative velocity profile between observation and calculation.

3.2. Inverse Problem Validation

As a known function, the density profile of bound vortex intensity on the blade camber line in Fig. 6a, which has been determined numerically in the direction problem at ϕ =0.154, was imbedded into a code which executes the inverse design of blade to identify if the inverse singularity method proposed is feasible or not. As result of this, a converged blade camber line of 70 iterations is shown in Fig. 6b. For that case, the relative error of warping angle actually is 9.94×10^{-4}, slightly less than the tolerance 1×10^{-3}. The original blade camber line precise restoration confirms the inverse singularity method and corresponding numerical scheme are correct and feasible.

3.3. Impeller Redesign

According to Fig. 5, at the design duty, a poor relative velocity profile is demonstrated on the blade pressure side in the original impeller. The drawbacks in the profile are that the peak loading is not only too close to the blade leading edge but also quit near the threshold. In that case, the hydraulic performance and suction characteristics of original impeller may be unsatisfactory, especially at partial flow rate. It is highly on demand to improve the impeller design. Two measures are taken hereby: (1) put more blades into impeller passages to lower the loading coefficient level, (2) move the peak loading coefficient away from the leading edge to somewhere close to the blade trailing edge. In doing so, the number of blades is increased to 5 from 4, and the density profile of bound vortex intensity is updated as shown in Fig. 7, where the peak loading factor has been moved to a position beyond the middle of blade camber line, i.e. r/r_2 =0.78. The peak value of the density has been lowered as low as 17m/s.

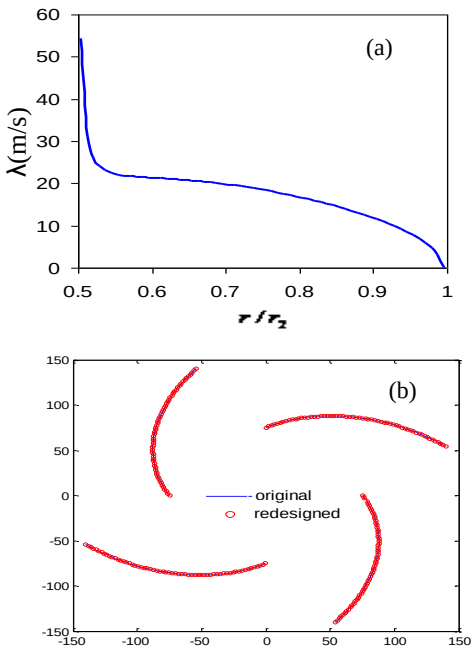

Figure 6.Known density profile of bound vortex intensity (a) and comparison of blade camber line between original and inversely designed impellers (b).

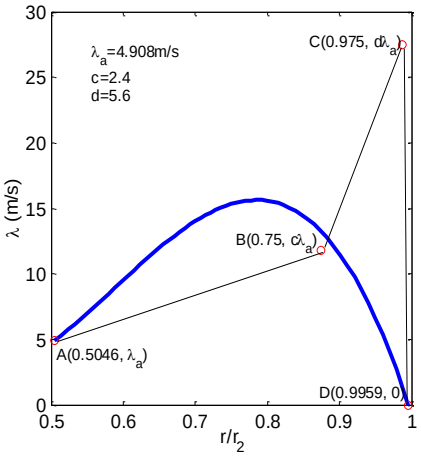

Figure 7.Modified density function of bound vortex intensity that is applied into inverse redesign of blade.

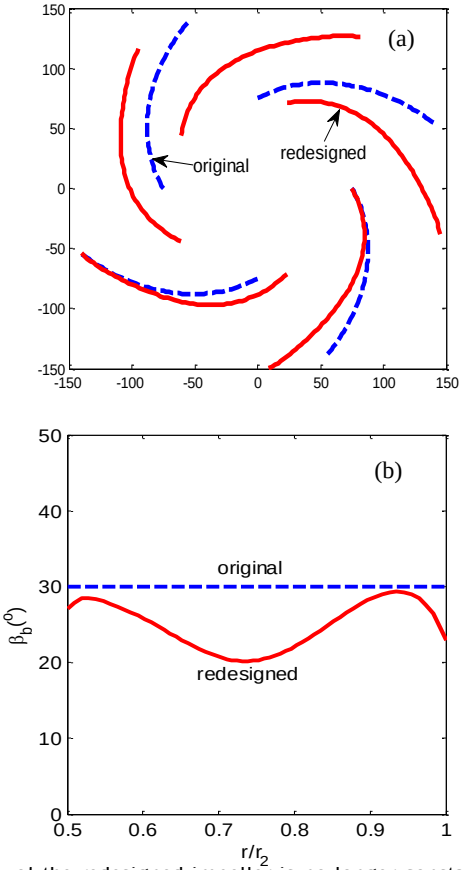

(b) of the

ade angle
e is made
es (86.6°
ade angle

of the redesigned impeller is no longer constant, but takes the shape of 'M'. The inlet and outlet blade angles are decreased to 27° and 22.9° from 30°, respectively. Accordingly, the angle of attack is reduced to just 2° from the initial 7°.

The estimated impeller performance is compared with that of the original one in Fig. 9a. At the design duty, the

theoretical head of original impeller is improved by 1m (water column height). The redesigned impeller is featured with a sharp negative slope head curve.

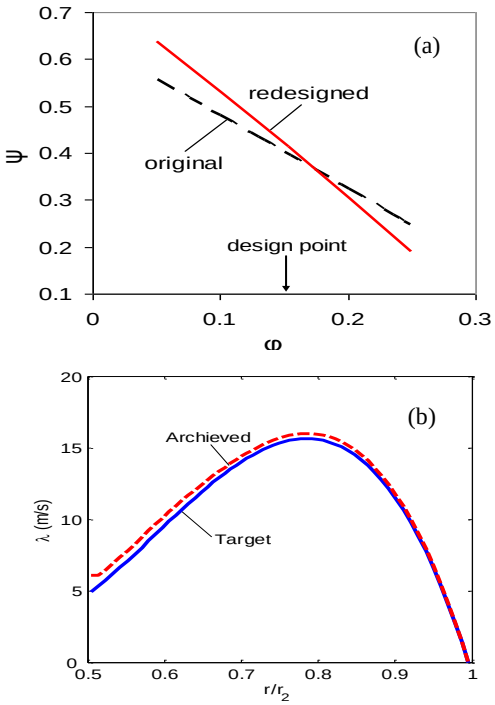

Figure 9.Impeller head coefficient (a) in terms of flow coefficient, target and achieved densities of bound vortex intensity (b).

prescribed and achieved densities of bound vortex intensity are illustrated in Fig.9b. The achieved density was evaluated based on the redesigned impeller as the direct problem. The difference in the density between two impellers does exist. It is increased towards the blade leading edge due to relatively severe bending of blade there. The maximum error is about 20% at the blade leading edge for there is a singularity point. The error is decreased to as low as 2.3% in the middle of blade length.

The blade loading coefficient is shown in Fig. 10a. Compared to Fig. 5b, the peak loading has been moved to the middle of blade length, r/r_2 =0.75, and the peak value is just 1.15, which is obviously less than a threshold of 2. Likewise, the relative velocity profiles on the blade surfaces are very satisfactory (Fig. 10b). The lowest velocity position has been moved to the middle of blade; moreover, its value is much larger than zero. For the redesigned impeller, its hydraulic performance, therefore, is superior to the original impeller, especially at partial flow rate (Fig. 9a). Note that the fluid is accelerated in the 65% blade camber line length long ($0.5 \le r/r_2 \le 0.82$) from the leading edge to a point beyond the middle of camber line on the suction side of the redesigned impeller. Such acceleration may suppress the growth of boundary layer on the blade suction surface, and may make positive contribution to reduction of hydraulic losses.

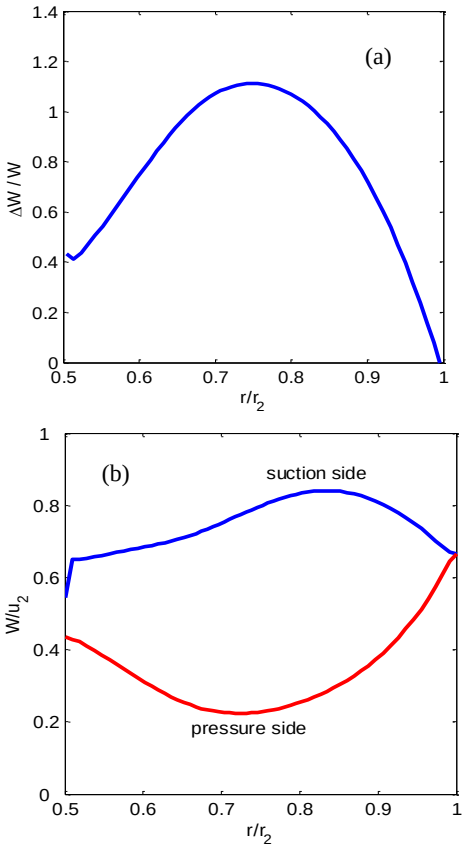

Figure 10.Loading coefficient (a) and relative velocity on blade surface (b).

3.4. CFD Conformation

3D solid geometry models of both the original and redesigned impellers have been generated by using Gambit. The 1/4 (original) and 1/5(redesigned) of the impellers are taken as the flow domain (Fig. 11), respectively. About 0.7 million tetrahedral cells are meshed and input into a CFD code Fluent to do flow simulations. In the simulations, the fluid is assumed to be steady, incompressible and turbulent. The standard $k-\varepsilon$ turbulence is activated to handle the turbulence effects. The non-equilibrium wall function is chosen to estimate wall shear stress and pressure more precisely. The detailed governing equations of flow, turbulence model and wall function can be found in Anonymous [15]. SIMPLE algorithm with the second-order up-wind scheme was applied to solve the governing equations. At the inlet to suction pipe, a normal velocity boundary is applied, which depends on flow rate. On the blade, shroud and hub, the velocity no-slip condition is held. At the outlet to impeller, zero pressure is given. The rest boundaries are subject to the periodic condition. The residual tolerance is 1×10^{-4}. The fluid is water at 20ºC.

  - Volume 5, Number 2 (ISSN 1995-6665)

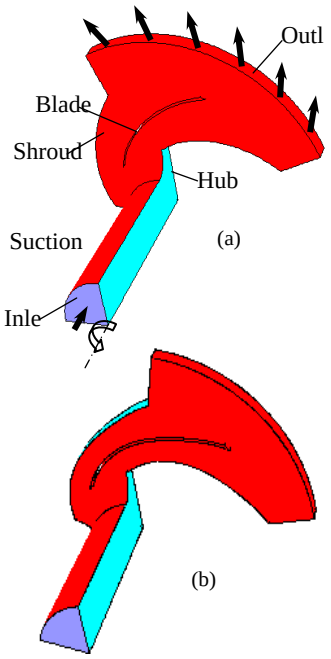

Figure 11.Flow domains of the original (a) and redesigned (b) impellers used in 3D flow CFD simulations.

The impeller theoretical head and hydraulic efficiency were extracted and are represented in Fig. 12 for the turbulent flow of viscous fluid. Obviously, the performance of the original impeller has been improved in great deal when the flow coefficient is in 0.025-0.16. At design duty ϕ =0.154, the hydraulic efficiency is raised by 5%, while the low flow coefficient ϕ =0.1, the efficiency is increased as high as 9%. These improvements suggest the blade loading control is necessary and takes a positive effect.

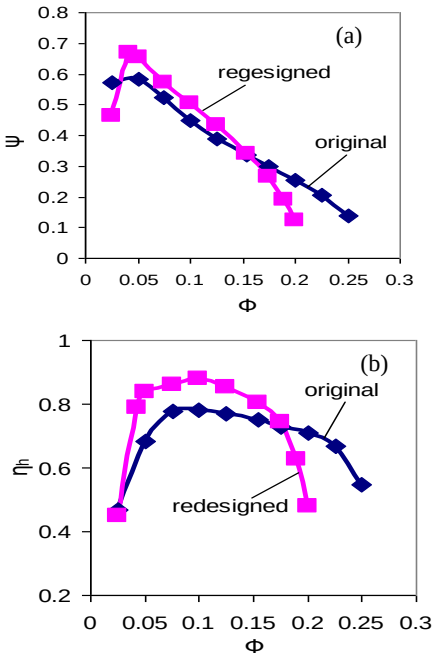

Figure 12. Head theoretical coefficient and hydraulic efficiency of the original (a) and redesigned (b) impellers calculated by CFD viscous fluid model

The relative velocity vector and pressure contour are displayed in Fig. 13 on the middle-span plane of the impellers for the viscous fluid flow. The reference pressure is 10m water column height. Even no significant evidence shows a reverse flow onset on the blade pressure side, it is noticed that a big zone with low velocity exists there in the original impeller. The blade pressure side of the impeller, especially, near the leading edge, is subject to much larger pressure compared to the redesigned impeller. Furthermore, the minimum pressure on the blade suction side in the original impeller is as low as -16.4m. In the redesigned impeller; however, it is just -5.46m.

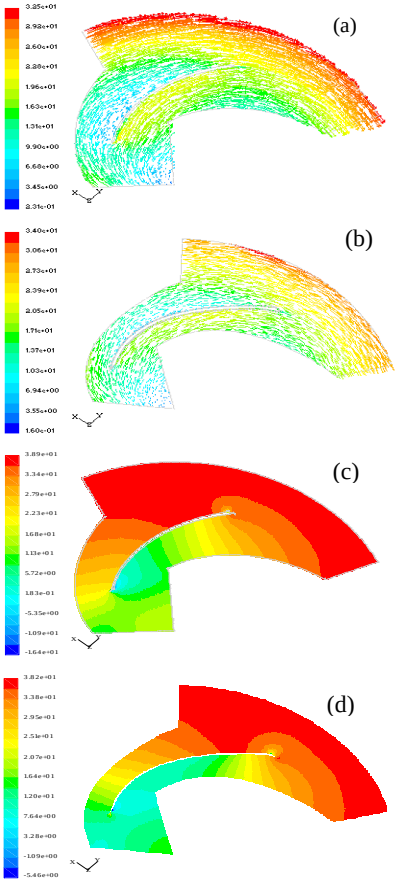

Figure 13.Relative velocity vector and static pressure contour of the original (a) & (c), redesigned (b) & (d) impellers calculated by CFD viscous fluid model.

The pressure on the blade pressure and suction sides and loading coefficient across the blade were extracted from the CFD results and are shown in Fig. 14 at the design condition. The pressure difference and loading coefficient across the blade in the original impeller is higher compared to the redesigned impeller, particularly, near the blade leading edge. Immediately after the leading edge the blade loading is kept to be nearly constant along blade in the original impeller; while it is increased until the beyond the middle of blade length, then decreased toward the trailing edge in the redesigned impeller. This suggests that the blade loading control in the inverse design is effective.

The loading coefficient magnitude and profile of 3D viscous flow are considerable different from those of 2D

potential flow shown in Fig. 5b. The reason for that is no viscous effect is involved in the potential flow model.

It is believed that the inverse singularity method can ensure an impeller to be able to achieve a better performance by using a carefully controlled density of bound vortex intensity on blade camber line. Such a method has a special significance in the redesign of existing centrifugal pump impellers.

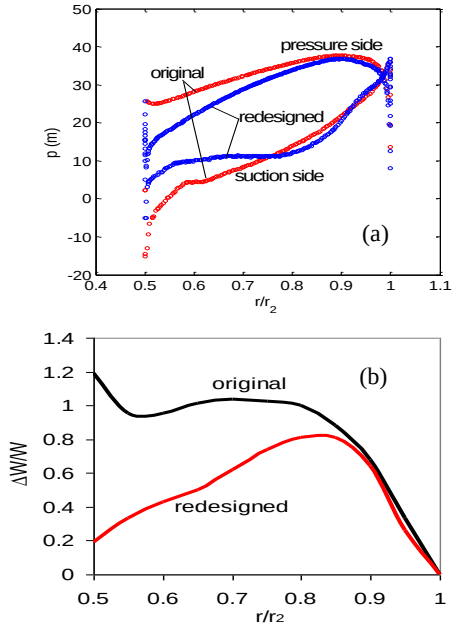

Figure 14.Pressure (a) and loading coefficient (b) on blade surface of the original and redesigned impellers in mid-span calculated by CFD viscous fluid model.

3.5. Discussion

The inverse singularity method proposed is subject to several limitations, for example, 2D, potential flow model; failure of handling viscous effect and secondary flow etc. Fortunately, these limitations can be removed by means of advanced CFD codes. For 2D blades, the blades can be established just on one S1 stream surface. For 3D twist blades, however, the blades should be designed on three or more S1 stream-surfaces. Theoretically, the current method is applicable for that case. However, how to specify density profile of bound vortex intensity along blade span needs to be investigated further. These S1 stream-surfaces of revolution can be determined by using the through-flow theory as indicated in Ghaly [16], Zangeneh [17], Borges [18], Peng et al [19]-[21].

Turbomachinery impeller blades can be established by using a given mean absolute velocity moment $V_u r$ in Borges [18], Peng et al [19]-[21], Tan et al [22], Luu et al [23], Jenkins and Moore [24], Dang and Isgro [25] and [26] or $\partial V_u r/\partial s$ in Ghaly [16] and Zangeneh [17], has long been recognized and realized. On a blade camber line, the density of bound vortex intensity λ is related to the velocity moment $V_u r$ with the following expression

$$\lambda = W_s - W_p = \frac{2\pi}{Z}\frac{\partial V_u r}{\partial s} \tag{22}$$

Since the prescribed $V_u r$ can be converted into λ, λ seems be equivalent to $\partial V_u r/\partial s$. In this contribution, λ's effect on the fluid flow in the impeller was taken into account by using analytical induced velocity equations. The considerable complicated mathematical contents have been removed. It is very hopeful such a simple method is acceptable for engineers.

4. Conclusions

An inverse singularity method was proposed for establishing the impeller blades of centrifugal pump in this article. A density distribution of bound vortex intensity on blade camber line was defined by using a cubic Bezier curve. The angle of attack has been involved in such a distribution. The results of the direct and inverse problems were validated by means of an experimental centrifugal pump impeller. The defined density of bound vortex intensity can ensure the designed blade to have a carefully controlled loading coefficient and smooth camber line to guarantee an improved hydraulic performance. The method may be applicable to the redesign of existing centrifugal pump impellers. Although a satisfactory outcome has been achieved yet for 2D blades, a further application to 3D twisted blades is highly desired. The prospective studies include 3D quasi-three-dimensional blade design and optimization of density profile of bound vortex tensity along blade camber line and span.

References

[1] K. Ayyubi, Y. V. N. Rao, "Theoretical analysis of flow through two-dimensional centrifugal pump impeller by method of singularities". ASME Journal of Basic Engineering, Vol. 93, 1971, 35-41.

[2] Y. R. Reddy, S. Kar, "Study of flow phenomena in the impeller passage by using a singularity method", ASME Journal of Basic Engineering, Vol. 94, 1972,513-521.

[3] T. Ogawa, S. Murata, "On the flow in the centrifugal impeller with arbitrary aerofoil blades (1st report, impeller with constant width)". Bulletin of the JSME, Vol. 17, No.108, 1974, 713-722.

[4] T. Ogawa, S. Murata, "On the flow in the centrifugal impeller with arbitrary aerofoil blades (2nd report, the effect of change in impeller width)", Bulletin of the JSME, Vol. 17, No. 108, 1974, 723-730.

[5] T. C. M. Kumar, Y. V. N. Rao, "Theoretical investigation of pressure distribution along the surfaces of a thin arbitrary geometry of a two-dimensional centrifugal pump impeller". ASME Journal of Fluids Engineering, Vol. 99, 1977, 531-542.

[6] T. C. M. Kumar, Y. V. N. Rao, "Quasi two-dimensional analysis of flow through a centrifugal pump impeller". ASME Journal of Fluids Engineering, Vol. 99, 1977,687-692.

[7] Betz, I. Flugge-Lotz, "Design of centrifugal impeller blades". NACA TM-902, 1939, 1-27.

[8] Y. Kashiwabaray, "Theory on blades of axial, mixed and radial turbomachines by inverse method". Bulletin of JSME, Vol. 16, No. 92, 1973, 272-281.

[9] S. Murata, Y. Miyake, K. Bandoh, "A solution to inverse problem of quasi-three-dimensional flow in centrifugal impeller". Bulletin of JSME, Vol. 26, No. 211, 1983, 35-42.

[10] Y. Senoo, Y. Nakase, "A blade theory of an impeller with an arbitrary surface of revolution", ASME Journal of Engineering for Power, Vol. 93, No. 4, 1971, 454-460.

[11] W. G. Li, "Analysis of flow in extreme low specific speed centrifugal pump impellers with multi-split-blade". International Journal of Turbo & Jet Engines, Vol. 23, No. 2, 2006, 73-86.

[12] Rogers D. F. An introduction to NURBS. San Francisco: Morgan Kaufmann Publisher, 2001.

[13] O. E. Balje, "Loss and flow path studies on centrifugal compressors-Part I", ASME Journal of Engineering for Power, Vol. 92, No. 2, 1970, 275-286.

[14] G. Kamimoto, K. Hirai, "On the flow in the impeller of centrifugal type hydraulic machinery (1st report)". Transaction of JSME, Vol. 19, No. 85, 1953, 37-43.

[15] Anonymous, FLUENT 5 User's Guide, Volume 4. Lebanon: Fluent Incorporated, 1998.

[16] W. S. Ghaly, "A design method for turbomachinery blading in three-dimensional flow". International Journal for Numerical Methods in Fluids, Vol. 10, No. 2, 1990, 179-197.

[17] M. Zangeneh, "A compressible three-dimensional design method for radial and mixed flow turbomachinery blades". International Journal for Numerical Methods in Fluids, Vol. 13, No. 5, 1991, 599-624.

[18] J. E. Borges, "A proposed through-flow inverse method for the design of mixed-flow pumps". International Journal for Numerical Methods in Fluids, Vol. 17, No. 12, 1993, 1097-1114.

[19] G. Y. Peng, S. L. Cao, M. Ishizuka, S. Hayama, "Design optimization of axial flow hydraulic turbine runner: Part I—an improved Q3D inverse method". International Journal for Numerical Methods in Fluids, Vol. 39, 2002, 517–531.

[20] G. Y. Peng, S. L. Cao, M. Ishizuka, S. Hayama, "Design optimization of axial flow hydraulic turbine runner: Part II-multi-objective constrained optimization method". International Journal for Numerical Methods in Fluids, Vol. 39, 2002, 517–531.

[21] G. Y. Peng, "A practical combined computation method of mean through-flow for 3d inverse design of hydraulic". ASME Journal of Fluids Engineering, Vol. 127, No. 6, 2005, 1183–1190.

[22] S. Tan, W. R. Hawthorne, C. Wang, J. E. McCune, "Theory of blade design for large deflections: Part II-annular cascades". ASME Journal of Engineering for Gas Turbine and Power, Vol. 106, 1984, 354-365.

[23] T. S. Luu, B. Viney, L. Bencherif, "Turbomachine blading with splitter blades designed by solving the inverse flow field problem". Journal of Physics III France, Vol. 2, 1992, 657-672.

[24] R. M. Jenkins, D. A. Moore, "An inverse calculation technique for quasi-three-dimensional turbomachinery cascades". Applied Mathematics and Computation, 57, 1993, 197-204.

[25] T. Dang, V. Isgro, "Euler-based inverse method for turbomachine blades part 1: two-dimensional cascades". AIAA Journal, Vol. 33, No. 12, 1995, 2309-2315.

[26] T. Dang, V. Isgro, "Euler-based inverse method for turbomachine blades part 2: three-dimensional flows". AIAA Journal, Vol. 38, No. 11, 1995, 2007-2013.